Structural and bioactivity evaluation of molybdenum-doped phosphate glasses: drug delivery application

Amira Fayad (amirafayad@gmail.com)
National Research Centre
Gehan El-Bassyouni
National Research Centre
Manal Abdel-Baki
National Research Centre
Manar Ahmed
National Research Centre

Research Article

Keywords: Bioactivity, Boro-phosphate glass, Drug delivery, Molybdenum oxide, Release Models, Structural properties

Posted Date: April 21st, 2022

DOI: https://doi.org/10.21203/rs.3.rs-1554213/v1

Abstract

Boro-phosphate glasses of stoichiometric chemical formula of (50-x)P_2O_5-20B_2O_3- 20CaO-10Na_2O (x = 5–15 mol. % MoO_3), have been prepared using melt-quenching technique. Structural and bioactivity properties of these glasses were considered. The bioactivity was evaluated upon 14 days of soaking in simulated body fluid (SBF) using: XRD, FT-IR and SEM. Through these techniques the creation of the calcium phosphate biolayer as one of the transitional yields of biomineralization is affirmed. Moreover, glass samples were examined as a drug delivery for ciprofloxacin (CIP) antibiotic. It was noticed that the higher the MoO_3 content the faster was the drug release rate. Textural analysis elucidated that by increasing the content of MoO_3, the surface area was increased. Mathematical models help to design a controlled drug release system. CIP in vitro release mechanism was determined by fitting different dissolution data into two different release models Zero Order and Higuchi model.

Introduction

Boro-phosphate based glasses are classified as an interesting class of multicomponent glass materials. They possess properties highly differ of pure borate and phosphate glasses that recommended them for potential applications of varied fields, from fast ion conductors such as fuel cells and gas sensors, glass solders of low melting point, hermetic sealing materials to biomaterials [1, 2]. Recently, bioactive glasses have attracted considerable attention for several causes, their bioactivity properties can be controlled through regulating the composition. In addition, they are absorbable; the glass structure progressively dissolves in human body through the development of hydroxyapatite (HA) coating on the external surface of glass [3].

Designed for bone tissue engineering, Phosphate glasses were used as a filler material for bone and manufactured scaffolds owing to their great solubility and chemical resemblance to the inorganic phase of the humanoid figure [4]. CaO and Na_2O are the main modifier oxides added to nearly all phosphate-based glasses to manage the solubility degree of glass in physiological environment [5]. The dissolution of Ca^{2+} ions from the glass gives rise to the creation of a CaO-P_2O_5 rich layer which end with the formation of hydroxyapatite [HA, $Ca_{10}(PO_4)_6(OH)_2$] [6]. On the other hand, glass composition with Na^+ ions cause effective flux in the glass melting process, by assisting the homogenizing and casting of glass [7]. Recent studies on compositions containing B_2O_3 informed the catalytic effect of boron atoms, which improves the bioactivity of glasses through their ability to form hydroxycarbonate apatite when dipped simulated body fluids (SBF) [8–11].

The influence of diverse elements which can be dissolved in the glass structure on the in vitro and/or in vivo properties has been investigated [10, 12–15]. Molybdenum (Mo) is one of the essential nutrients for our body; because of its unique chemistry, it is necessary for specific functions [16]. It is a transition metal found in the body in either the Mo^{4+} or Mo^{6+} valence state bound to sulfur or oxygen. In oxidation-

reduction reactions, molybdenum easily changes the oxidation state, it functions as an electron transfer agent [17].

In the current study, glass samples of stoichiometric chemical formula of (50-x)P_2O_5-20B_2O_3- 20CaO-10Na_2O (where x = 5, 10, 15 mol. % MoO_3) have been prepared. Special care was paid to the glass structural characterization and bioactivity upon soaking in SBF for 14 days using XRD, FTIR and SEM techniques. Likewise, drug loading efficiency, and in vitro release of the CIP-loaded glass was considered attaining operative antibiotic therapy. Ciprofloxacin (CIP) antibacterial drug was nominated as a drug model in this study because of its broad-spectrum antibiotic ability to treat severe infections, which may be accompanying the claim of bone-filling materials, bone replacements or orthopedic implants.

Experimental Procedure

2.1. Glass Preparation

The samples of phosphate-based glass have been prepared with different oxides starting from analar grades NaH_2PO_4, $CaCO_3$, Na_2CO_3, H_3BO_3 and MoO_3. The required quantities of the above components were quietly mixed then heated in a platinum crucible to 700°C in an electrically muffled furnace for two hours with continues stirring the melt to remove H_2O, NH_3 and CO_2 completely. The melted samples were held at temperature of 1000°C for 30 min. The melts were cast into slightly warmed stainless-steel molds, and the collected prepared glassy samples were immediately transferred to a muffle regulated at 350°C for annealing. The muffle was switched off after 1 h and left to cool at a rate of 25°C/h.

2.2. Characterization Protocol

The infrared absorption analysis was measured using a Fourier transform infrared spectrometer (JASCO FTIR-430, Japan) at room temperature in the range 400-4000 cm^{-1}. The measured samples previously prepared by mixing their fine powder with dried KBr in the ratio 1:100, and the mixture was subjected to a load of 5 tons/cm^2 in an evocable die for 2 min to produce clear homogeneous disks ready to the FT-IR measure immediately. To interpret the spectra obtained, the region of 400-1800 cm^{-1} has been chosen.

X-ray diffraction (XRD) were measured by the crushing samples into fine powders using pestle and mortar. XRD analysis was performed using diffractometer with Cu radiation (λ =1.5405 Å) operating at 40 kV, 30 mA at room temperature. Diffraction patterns were acquired on finely ground samples for 2θ values ranging from 5 to 80 degrees

The surface morphology of glass samples was scanned with a scanning electron microscope, SEM model Philips XL30 using an accelerating voltage of 30 kV, and a wavelength resolution of 3.5 nm. To perform the SEM measurements the samples were glued on the sample holder with conductive carbon cement and then coated with gold using Edwards S 150 sputter coater device.

2.3. SBF Preparation and In-Vitro Bioactivity Inspection

Simulated body fluid was prepared following the Kokubo technique **[18],** which is the closest to the human blood plasma regarding to the concentration of ions, buffered at pH = 7.38 by tris–hydroxymethyl-aminomethane (Tris, 50 mM) and 1 M hydrochloric acid (HCl). The ability of the prepared samples to create the hydroxyapatite layer on their surface was inspected through immersing 0.5 gm from the powdered sample in clean bottles filled with (25 ml) of SBF, stored in a thermostat at 37°C for 14 days. After that, the samples were filtered, rinsed with doubly distilled water and dried in air at room temperature. The variations occurred on the surface were studied through SEM, XRD and FT-IR measurements.

2.4. Drug Delivery Application

In 2019 Permanadewi et al. **[19]**, clear that the drug release system is a method in which a bioactive constituent discharged from a drug product and go in the process of distribution and absorption to provide its pharmacological action. The drug release is preserved at a definite rate to exploit the benefits as well as to conquer the side impacts **[19].** Drug release is governed by few intrinsic properties of the glassy matrix such as molecular weight, drug solubility, and matrix swelling.

2.4.1. Drug Loading into the Glass

There are three types of drugs used to treat osteomyelitis: gentamicine sulfate, vancomycin hydrochloride and ciprofloxacin. Ciprofloxacin (CIP) is an antibiotic that is useful in treating many bacterial infections. It is a second-generation fluoroquinolone. The spectrum of its activity includes most strains of bacterial pathogens responsible for infections of respiratory system, urinary tract, gastrointestinal, and abdomen. Therefore, it was used as a model drug in the current study. The structure of ciprofloxacin is shown in the **Fig. (1).**

Ciprofloxacin solution of concentration 1 mg/ml was prepared. Glass samples were immersed in 8 ml of the drug solution at 37°C for 2 days and left to dry for 4 days. The drug solution was then removed. The uptake of drug by glass sample was calculated as the difference in drug concentration before and after immersion. The drug loading and the amount of CIP entrapped in the glass mat was measured by UV/Visible spectrometer (Model, SP-2000 UV) at wavelength of 277 nm.

2.4.2. Determination of the Cumulative Drug Released from the Glass

Each drug loaded glass sample was immersed in 8 ml tris buffer solution, then the solution was withdrawn, and replaced by fresh tris buffer after different time periods. In order to measure the concentration; eluted samples were frozen at - 4°C. The amounts of ciprofloxacin released were measured using a UV spectrophotometer at λ = 277 nm. In addition, standard solutions of known drug concentration were prepared and tested by the same method to calculate the unknown drug concentrations in the samples.

2.5. Textural Analysis of Glass Nanoparticles

Nitrogen adsorption–desorption isotherms were measured with a high-speed gas sorption analyzer (NOVA 2000 series, chromatic, UK) at 77 K. Before measurements, samples were out-gassed at 150°C in vacuum for 6 h. The Barrett–Emmett–Teller (BET) method was utilized to calculate the specific surface areas. The average pore diameter and pore-size distributions were derived from the adsorption branches of the isotherms using the Barrett–Joyner–Halanda (BJH) method. The total pore volume was estimated from the amount adsorbed at a maximum relative pressure.

Results And Discussion

3.1. FTIR Analysis Before and After Immersion

Fig. (2) Illustrates the FTIR spectral curves of the undoped glass together with that for Mo_2O_3 – doped glass samples in the mid IR range of 400-1800 cm^{-1}. Whereas the Infrared spectroscopy (IR) is used to attribute the observed absorption peaks to the suitable vibration of the atoms in geometric grouping for well understanding the structure and dynamics of glass matrix. The FTIR spectra show two broad bands cover the wavenumber ranges 400-700 and 700-1300 cm^{-1} besides the peaks at 1380, 1450, 1621 and 1722 cm^{-1} therefore the FTIR spectra have been deconvoluted to identify the overlapped or concealed IR peaks for the various glass network building units. Therefore, the resultant FTIR data can be assigned as follows:

(a) The FTIR absorption peaks located at 444 and 540 cm^{-1} are correlated to the bending oscillation of bridging phosphorus such as O□P–O and/or O–P–O **[20, 21]** in PO_3, PO_4, and P_2O_7 phosphate species **[22]**.

(b) The peak around 719 cm^{-1} may be allocated to bending oscillation of B–O–B linkages and symmetric stretching of the P–O–P linkages vibration modes of bridging oxygen.

(c) The spectral peaks positioned at 893 is attributed to asymmetric stretching oscillations of P-O-P within boro-phosphate glass **[23, 24],** though frequency at 966 cm^{-1} can be due to the vibration way of the isolated $(PO_4)^{3-}$ tetrahedral units **[25],** the asymmetric stretching oscillation of P–O–P bond **[24]** or the symmetric stretching vibration of (PO_3) units of Q^1 structural species **[24, 25]**.

(d) The spectral bands identified around 1029 cm^{-1} reflects both the asymmetric stretching oscillation of PO_3^{2-} in Q^1 species besides stretching oscillation of B-O in BO_4^- **[23-25],** while the frequency at 1115 cm^{-1} plus 1161 cm^{-1} are assigned to symmetric stretching vibration of $(PO_2)^-$ in Q^2 phosphate units and B-O in BO_4 species **[25]**.

(e) The IR absorption bands occurred at 1386 and 1440 cm^{-1} could be attributed to

B–O stretching oscillations of $(BO_3)^{3-}$ species in pyro-, meta- and ortho-borate linkages, as well as to the P=O asymmetric stretching vibration of meta-phosphate (PO_2) species **[26].**

(f) The OH links, H-O-H of water molecule or P-OH bending vibration are assigned spectral bands at 1621 and 1716 cm^{-1} **[27]**.

The impact of molybdenum oxide on the glass structure is obviously observed at the widely broad band covering the wavenumber in the range from 800 -1500 cm^{-1}. This band is indeed splitting into three IR spectral ranges positioned at 800–1000 cm^{-1}, 1000–1300 cm^{-1} and 1300- 1500 cm^{-1} with more pronounced absorption peaks than that detected in the base glass spectrum. Molybdenum ions could be Mo^{6+} and Mo^{5+} within the glass network, get in the matrix as former and modifier when associated with four or six oxygen creating tetrahedral MoO_4 and octahedral MoO_6 structural species. Molybdenum ions revealed infrared absorption with vibration bands at about 920–900, 850–830, 800 and 430–410 cm^{-1}. as well as asymmetric and symmetric oscillations of Mo-O-Mo links can be observed at about 600 and 450 cm^{-1}, respectively as confirmed through various studies on molybdate glasses **[28-31]**. Through these findings, the existence of the spectral infrared peak at about 840 cm^{-1} in 5-Mo and 10-Mo glasses and at about 912 cm^{-1} in 15-Mo glass elucidates the contribution of molybdenum ions within the glass lattice as an insulated MoO_4 tetrahedron. In addition, the appearance of absorption peak around 622-614 cm^{-1} and 440-435 cm^{-1} with increase the molybdenum content is credited to asymmetric vibration of the Mo-O-Mo linkage. Besides the absorption peaks appeared around 1313 and 1253 cm^{-1} are ascribed to asymmetric stretching oscillations of nonbridging oxygen of P-O-P in phosphate chains **[32]** and to both asymmetric stretching vibration of PO^{2-} in Q^2 units and asymmetric stretching vibration of $BØ_3$ and $BØ_2O^-$, respectively **[25-26]**. beside the bands at around 1102 and 889 cm^{-1} are reduced, demonstrating a raise in the pyro-phosphate as well as BO_3 units. In addition, the intensity of the spectral band around 963 cm^{-1} increased and shifted to shorter wavenumber. From FTIR results it is well-known that, the intensities of altered vibration bands of phosphate structures improved by rise in the content of MoO_3. Such oxide operated as an ionic cross-linker among non-bridging oxygens (NBOs), and consequently, intensify the ionic bond strength and reduce the P–O bonds. Therefore, Mo ions generate Mo–O–P and Mo–O–B bonds through its modifying action that depolymerize the phosphate chains **[28]**.

The FTIR vibration spectra of the immersed parent glass together with the doped samples reveals more simplified IR features than that of the same glasses before immersion and the combined multi-vibrational bands was diminished **(Fig. 3).** The FT-IR spectral modes are related to P-O vibration that associated with the creation of the calcium-phosphate layer upon immersion in SBF **[33]** that declare the development of apatite layer. The more prominent bands in the far-IR range (440-735) cm^{-1} located at 549 and 665 cm^{-1} and shifted to 565 and 646 cm^{-1} with high content of MoO_3 can be ascribed to the P-O bending vibrations **[33]**. The intensity of the spectral peak in the range (1033-1039) cm^{-1} growth with the increase of MoO_3 content that may be assigned to PO_4^{3-} vibrations, characteristic for calcium phosphate phase. The high intensity peak at around 1149 cm^{-1} is correlated to the corrosion process involving the development of P–OH instead of P–Na or parallel units **[27]**. Additionally, the band identified at about 1633 cm^{-1} is due to

v_3–vibrations of CO_3^{2-} units **[34]**. These bands all in all are representative for the calcium phosphate phase ($Ca_3(PO_4)_2 \cdot xH_2O$) **[34].**

3.2. XRD Spectroscopy

Figure (4) shows the XRD pattern of the studied glasses before immersion in SBF. It exhibits a broad band with no eminent sharp peaks. Such XRD features are certainly consistent with amorphous (un-structured) nature of the glass samples.

Fig. (5) Illustrates the XRD on the glass surface after immersion for 14 days in SBF. The X-ray diffraction spectra shows a main calcium phosphate phase of formula calcium pyrophosphate ($Ca_2P_2O_7$, CPP) in the range of 2θ (25-35) ^{o} as one of the intermediate products in the biomineralization process corresponding to JCPDS card no. 17-0499 **[35]**.

3.3. SEM spectroscopy

Fig. (6) Shows the SEM micrographs of the surface morphology of the as-prepared glasses and all post immersed glass samples in SBF for 14 days. By comparing the SEM image before and after 14 days immersion in SBF is easy to point out morphological changes. The development of the apatite layer goes through two stages. Starting with the foundation of the amorphous calcium phosphate (ACP) coating and then finally converting to crystalline apatite **[33]**. As depicted from **Fig. (6),** glass shows no identified crystalline phases before immersion. However, there are different morphological features on the surface of the immersed samples thus indicating the creation of calcium-phosphate biolayer. The characterized rounded or nodular shaped of the bioactive apatite micro-species can be clearly identified on the most surface of the immersed samples and it is more developed as MoO_3 content increase. Therefore, it can be observed that the addition of MoO_3 strengthens the growth of HA layer so enhancement the bioactivity of the studied glass samples. This result is in harmony with the FTIR results.

3.4. Glass Surveying as a Delivery System for Ciprofloxacin

3.4.1. Loading of Drug onto Glass

Ciprofloxacin (CIP) is one of the Biopharmaceutics Classification System (BCS) Class II/IV drugs, which is an antibiotic of broad-spectrum, second-generation fluoroquinolone **[36]. Fig (7)** displays the loaded amount of ciprofloxacin onto each glass sample which indicated that CIP was successfully loaded onto the glass and could be released **[37]**. It is proposed that CIP was positively loaded onto the glass samples. This was recognized because of the occurrence of the P_2O_5 oxides in the glass matrix. Upon hydrolysis, such oxide was identified to form POH groups which could form hydrogen bonding with the drug molecules and as a result improved the CIP loading onto the glass **[38].**

3.4.2. In vitro Drug Release Profile

Fig. (8) shows the ciprofloxacin (CIP in %) cumulative release profile from the glass samples as a function of time. The profile release of drug exhibited a preliminary fast release stage followed by slower successive release stage. The transition to the second stage occurred at 12 hours and continued throughout the end of the releasing period up to 28 days (i.e., 700 hours) which may be accredited to the slow diffusion of the CIP molecules held inside the glass structure. It can be observed that the higher the MoO_3 content the faster the drug release rate, that can be related to the nonbridging oxygens development and negative charge potential with molybdenum content increase. It was revealed that Mo^{5+} ions depolymerize the glass matrix by forming further bonding defects and molybdenum ions Mo^{6+} can exist in fourth-fold coordination, resulting in loose and more opened glass network **[39].** In addition, molybdenum has a smaller ionic field strength than some other elements such as vanadium, so the dipole effect is weaker and therefore the negative charge effectiveness is smaller on oxygen for hydrogen bonding. Therefore, the Mo-O bond forms a weak hydrogen bond upon contact with drug functional groups as confirmed by El-Meliegy et al **[39]**. Thus, a continuous drug release profile was attained by using glass samples doped with Mo_2O_3 as delivery vehicle for ciprofloxacin **[40].**

3.5. Textural Analysis:

Fig. (9) Elucidates the N_2 adsorption isotherms of glass samples. They correspond to the type IV isotherm agreeing to the arrangement of the IUPAC. In the samples, the representative hysteresis loop of this isotherm could be detected [at relatively high P/P_0 values, the desorption branch did not monitor the same route as that of the adsorption one]. This performance evidently designated the existence of mesopores according to the IUPAC classification **[41]**.

The allocation of pore size attained from the desorption branch of the isotherm following the BJH method for all samples are shown in **Fig. (10).** Moreover, all samples showed monomodal pore size distribution. **Table 1** summarizes all data of the textural analysis for all samples. It could be seen that the addition of MoO_3 was in charge of the decrease in the surface area of the MoO_3 modified samples as compared with the control. However, by increasing the MoO_3 content, the surface area was increased, as the modifier molybdenum enters the glass system which make it more connected. Furthermore, the high surface area could enable the dispersion of drug solution into the glass interior structure through the loading period. Additionally, glass could congregate the drug molecules inside their pores and perform as reservoirs for the drug.

Table 1: The data of the textural analysis carried out for studied glass samples

Glass sample code	0-Mo	5-Mo	10-Mo	15-Mo
Surface area	0.89	0.15	0.29	0.45
Average pore diameter (nm)	5.94	4.51	5.88	4.91
Total pore volume ($cm^3\ g^{-1}$)	1.33E-03	1.75E-03	4.32E-04	5.58E-04

3.6. The Kinetics of Cumulative Drug Released

To study the in vitro release kinetics, the drug released cumulative percent was plotted against time in hours. The in vitro release mechanism of ciprofloxacin was determined by fitting the dissolution data into two mathematical release models: Zero Order and Higuchi models of fitting **[42, 43]**. The kinetic equations, and regression coefficient, R^2, were used as a suggestion of data fitting.

To investigate the kinetics of the released drug, we alienated curve in **Fig (8)** into two parts. First part was solved by zero order model and the second part by Higuchi model fitting. For zero-order release kinetics, the dissolution of a drug is merely a function of time. Such model is accurate in case of very slow drug release. The regression coefficient (R^2) and kinetic equations are used as a clue of data fitting. In order to decide which model is appropriate for the drug release kinetics, the regression coefficients (R^2) were considered by means of regression analysis. The diverse kinetic equations are zero order drug release model which deliberate the process of constant drug released from the drug delivery device and other delivery system suggested by equation (1):

$$Q_t = Q_0 + K_0\, t \qquad (1)$$

Where, Q_t is the quantity of drug released in time t, Q_0 the original amount of drug in sample solution and K_0 is the zero-order constant.

On the other hand, the second model Higuchi is the relation between drug release concentration (%) and the square root of time ($t^{0.5}$), to study the release of water soluble and poorly soluble drugs from variable matrices represented by Eq. 2:

$$Q_t = K_H t^{0.5} \qquad (2)$$

Where, K_H is the Higuchi release rate constant. To clarify the mechanism of drug release, and to find a suitable model for drug release kinetics; the regression coefficient (R^2) was calculated from the curve, in the present study; R^2 was greater than 0.9 [i.e., it is significant to such model fitting]. Hence, it could be concluded that the regression coefficient (R^2) of the *in vitro* release profile for ciprofloxacin drug could be best uttered by zero order and Higuchi models fitting ($R^2 > 0.9$).

Conclusions

Glass doped with variable molar percent of MoO_3 have been prepared via melt-quenching technique. XRD features are certainly consistent with the amorphous nature of the glass. FT-IR spectra data show the existence of phosphate groups sharing with borate units. The amending action of molybdenum ions depolymerize these chains and generate both Mo–O–P and Mo–O–B bonds. Bioactivity after soaking in SBF for 14 days was examined using XRD, FTIR and SEM techniques. XRD shows a main calcium phosphate phase of calcium pyrophosphate as one of the transitional products in the biomineralization.

IR spectra of the immersed glasses display bands matching with P-O vibrations accompanying the formation of the calcium phosphate layer, which affirm the development of an apatite layer on the surface of the immersed glass. Also, different morphological feature was identified on the surface of the immersed glass using SEM. Such feature indicates the creation of calcium-phosphate biolayer. The characterized rounded or nodular shaped of the bioactive apatite micro-species was clearly identified on the surface and it was more developed as the MoO_3 content increase. Therefore, it can be observed that the addition of MoO_3 supports the growth of HA layer thus improving the bioactivity of the studied glass. Moreover, glass samples were examined as a drug delivery for ciprofloxacin antibiotic drug. Results proved that ciprofloxacin was positively loaded onto the glass samples as a result of the occurrence of the P_2O_5 oxides in the glass matrix. Besides, the higher the MoO_3 content the faster was the drug release rate from the glass. Mathematical models help to design a controlled drug release system. It was noticed that the higher the MoO_3 content the faster was the drug release rate. That could be attributed to the following supposition: by increasing the molybdenum content, the glass network was opened and that is why the drug was released faster. In vitro release mechanism of ciprofloxacin drug was inspected by fitting different dissolution data into two mathematical kinetics release models, Zero Order and Higuchi model fitting. As the calculated regression coefficient (R^2) is higher than 0.9, hence it could be decided that the in vitro release profile for ciprofloxacin drug could be best uttered by zero order and Higuchi models fitting. In conclusion, the rate of drug release can be directed to deliver the drug molecules over several weeks.

Declarations

Conflict of interest

The authors declare that they have no known competing financial interests or personal relationships that could have appeared to influence the work reported in this paper.

Acknowledgements

This research did not receive any specific grant from funding agencies in the public, commercial, or not-for-profit sectors. The scientific facilities of the National research Centre (NRC) have been used to investigate this research.

Authorship contribution statement

A. M. Fayad: Methodology, Investigation, Writing – review & editing.

Gehan T. El-Bassyouni: Methodology, Investigation, Writing – review & editing.

M. Abdel-Baki: Methodology, Investigation, Writing – review & editing.

M. M. Ahmed: Methodology, Investigation, Writing – review & editing.

References

1. A.N. Cormack and A. Tilocca Structure and biological activity of glasses and ceramics, Phil. Trans. R. Soc. A 370 (2012) 1271-1280.
2. R. Lucacel Ciceo, M. Todea, R. Dudric, A. Buhai, V. Simon, Structural effect of cobalt ions added to a borophosphate-based glass system, J. Non-Cryst. Solids 481 (2018) 562-567.
3. J.R. Jones, L.M. Ehrenfried, L.L. Hench, Optimizing bioactive glass scaffolds for bone tissue engineering. Biomaterials27 (2006) 964-973.
4. M. Uo, M. Mizuno, Y. Kuboki, A. Makishima, F. Watari, Properties and cytotoxicity of water soluble Na_2O-CaO-P_2O_5 glasses, Biomaterials 19(24) (1998) 2277-2284.
5. A. Maheswaran, G. Hirankumar, N. Heller, S. Karthickprabhu, J. Kawamura, Structure, dielectric and bioactivity of P_2O_5–CaO–Na_2O–B_2O_3 bioactive glass, Appl. Phys. A 117 (2014) 1323-1327.
6. L.L. Hench, R.J. Splinter, W.C. Allen, T.K. Greenlee, Bonding mechanisms at the interface of ceramic prosthetic materials, J. Biomed. Mater. Res. 5(6) (1971) 117-141.
7. C.C. Lin, L.C. Huang, P. Shen, $Na_2CaSi_2O_6$–P_2O_5 based bioactive glasses. Part 1: Elasticity and structure, J. Non-Cryst. Solids 351(40-42) (2005) 3195-3203.
8. A. Saranti, I. Koutselas, M.A. Karakassides, Bioactive glasses in the system CaO–B_2O_3–P_2O_5: Preparation, structural study and in vitro evaluation, J. Non-Cryst. Solids 352(5) (2006) 390-398.
9. G. Kaur, G. Pickrell, G. Kimsawatde, D. Homa, H.A. Allbee, N. Sriranganathan, Synthesis, cytotoxicity and hydroxyapatite formation in 27-Tris-SBF for sol-gel based CaO-P_2O_5-SiO_2-B_2O_3-ZnO bioactive glasses, Sci. Rep. 4 (2014) 4392.
10. A. Hope, N.S. Gudal, Aldo R. Boccaccini, A review of the biological response to ionic dissolution products from bioactive glasses and glass-ceramics, Biomaterials 32(11) (2011) 2757-2774.
11. M.N. Rahaman, D.E. Day, B.S. Bal, Q. Fu, S.B. Jung, L.F. Bonewald, A.P. Tomsiac, Bioactive glass in tissue engineering, Acta Biomater. 7(6) (2011) 2355-2373.
12. Q. Fu, M.N. Rahaman, H. Fu, X. Liu, Silicate, borosilicate, and borate bioactive glass scaffolds with controllable degradation rate for bone tissue engineering applications. I. Preparation and in vitro degradation, J. Biomed. Mater. Res. A 95A (2010) 164-171.
13. S. Hami, G. Gorianc, L. Moimas, B. Lindroos, H. Huhtala, S. Raty, H. Kuokkanen, G.K. Sandor, C. Schmid, S. Miettinen, R. Suuronen, Characterization of zinc-releasing three-dimensional bioactive glass scaffolds and their effect on human adipose stem cell proliferation and osteogenic differentiation, Acta Biomater. 5 (2009) 3122-3131.
14. D.S. Brauer, M.N. Anjum, M. Mneimne, R.M. Wilson, H. Doweidar, R.G. Hill, Fluoride-containing bioactive glass-ceramics, J. Non-Cryst. Solids 358 (12-13) (2012) 1438-1442.
15. G. Lusvardi, G. Malavasi, L. Menabue, M.C. Menziani, U. Segre, Synthesis and in vitro studies of phosphosilicate glasses doped with cerium and zinc oxides, J. Appl. Chem. Biotech. 2 (3) (2004) 212.

16. R. Ciceo Lucacel, O. Ponta, E. Licarete, T. Radu, V. Simon, Synthesis, structure, bioactivity and biocompatibility of melt-derived P_2O_5-CaO-B_2O_3-K_2O-MoO_3 glasses, J. Non-Cryst. Solids 439 (2016) 67-73.
17. Vincent S. Gallicchio, in: Faik Atroshi (Ed.), Use of Trace Elements and Halotherapy in the Treatment of Human Diseases in Pharmacology and Nutritional Intervention in the Treatment of Disease (2014) 43-95.
18. T. Kokubo, H. Kushitani, S. Sakka, T. Kitsugi, T. Yamamuro, Solutions able to reproduce in vivo surface-structure changes in bioactive glass-ceramic A-W, J. Biomed. Mater. Res. 24(6) (1990) 721-734.
19. I. Permanadewi, A.C. Kumoro, D.H. Wardhani, N. Aryanti, Modelling of controlled drug release in gastrointestinal tract simulation, IOP Conf. Series: Journal of Physics: Conf. Series 1295 (2019) 012063.
20. Y. M. Moustafa, K. El-Egili, Infrared spectra of sodium phosphate glasses, J. Non-Cryst. Solids 240(1-3) (1998) 144-153.
21. A. M. Ibrahim, Structural, optical and electrical investigation of sodium phosphate glasses doped MoO_3 for high power visible laser safety, Mater. Chem. Phys., 252 (2020) 123237.
22. S. V. Stefanovsky, O. I. Stefanovsky, I. L. Prusakov, M. I. Kadyko, A. A. Averin, B. S. Nikonov, Speciation of sulphate ions in sodium alumino(iron)phosphate glasses, J. Non-Cryst. Solids 512 (2019) 81-89.
23. S. Agathopoulos, D. Tulyaganov, J. Ventura, S. Kannan, A. Saranti, M.A. Karakassides, J.M.F. Ferreira, Structural analysis and devitrification of glasses based on the CaO–MgO–SiO_2 system with B_2O_3, Na_2O, CaF_2 and P_2O_5 additives, J. Non-Cryst. Solids 352 (2006) 322–328.
24. M. Ouis, A. Fayad, A.A. Abd El Aty, G.T. El-Bassyouni, Processing, Characterization and Application of Some Borophosphate Glasses Containing Antibacterial and Antifungal Oxides in Bioactive Demands, Egypt. J. Chem. 61(1) (2018): 163-173.
25. R.L. Ciceo, M. Todea, R. Dudric, A. Buhai, V. Simon, Structural effect of cobalt ions added to a borophosphate-based glass system, J. Non-Cryst. Solids 481 (2018) 562-567.
26. R. Ciceo-Lucacel, T. Radu, O. Ponta, V. Simon, Novel selenium containing borophosphate glasses; preparation and structural study, Mater. Sci. Eng. C 39 (2014) 61-66.
27. A. M. Fayad, M. A. Marzouk, F. H. El-Batal, Bioactivity behavior of Ag_2O or CuO doped in glass systems of Na_2O–CaF_2–P_2O_5 and Na_2O–CaO–P_2O_5 and their glass–ceramic derivatives assessed by FTIR, X-ray diffraction and SEM measurements, SN Appl. Sci., 1(3) (2019) 203.
28. L. Bih, L. Abbas, A. Nadiri, H. Khemakhem, B. Elouadi, Investigations of molybdenum redox phenomenon in Li_2O–MoO_3–P_2O_5 phosphate glasses, J. Mol. Struct., 872 (2008) 1-9.
29. A.V.R. Kumar, C.S. Rao, G.M. Krishna, V.R. Kumar, N. Veeraiah, Structural features of MoO_3 doped sodium sulpho borophosphate glasses by means of spectroscopic and dielectric dispersion studies, J. Mol. Struct., 1016 (2012) 39-46.

30. F. H. El Batal, Gamma ray interaction with sodium phosphate glasses containing MoO_3, Nucl. Instrum. Methods in Phys. Res. B, 265 (2007) 521-535.
31. G. M. Turky, A. M. Fayad, G.T. El-Bassyouni, M. Abdel-Baki, Dielectric and electrical properties of MoO_3-doped borophosphate glass: dielectric spectroscopy investigations, J Mater. Sci: Mater Electron, 32 (2021) 22417–22428.
32. Wan Ming Hua, Wong Poh Sum, Rosli Hussin, Zuhairi Ibrahim, Structural Study on Lithium-Barium Borophosphate Glasses using Infrared and Raman Spectroscopy. Advanced Materials Research Vol. 626 (2013) pp 11-15 Online: 2012-12-27
33. K. Magyari, R. Stefan, A. Vulpoi, L. Baia, Bioactivity evolution of calcium-free borophosphate glass with addition of titanium dioxide, J. Non-Cryst. Solids 410 (2015) 112-117.
34. P. Sobhanachalam, V. Ravi Kumar, N. Venkatramaiah, Y. Gandhi, N. Veeraiah, Synthesis and in vitro characterization of cerium oxide mixed calcium oxy fluoro borophosphate bioactive glasses by means of spectroscopic studies, J. of Non-Cryst. Solids 498 (2018) 422-429.
35. A. M. El-Kady, K.R. Mohamed, G.T. El-Bassyouni, Fabrication, characterization and bioactivity evaluation of calcium pyrophosphate/polymeric biocomposites, Ceram. Int., 35 (2009) 2933-2942.
36. H.D. Williams, N.L. Trevaskis, S.A. Charman, R.M. Shanker, W.N. Charman, C.W. Pouton, C. J. H. Porter, Strategies to Address Low Drug Solubility in Discovery and Development. Pharmacol. Rev. 65 (2013) 315-499.
37. A. M. El-Kady, M. M. Ahmed, B.M. Abd El-Hady, A. F.Ali, A.M. Ibrahim, Optimization of ciprofloxacin release kinetics of novel Nano-bioactive glasses: Effect of glass modifier content on drug loading and release mechanism, J. of Non-Cryst. Solids 521 (2019) 119471.
38. A.M. El-Kady and M.M. Farag, Bioactive Glass Nanoparticles as a New Delivery System for Sustained 5-Fluorouracil Release: Characterization and Evaluation of Drug Release Mechanism, J. Nanomater. Volume 2015 (2015) Article ID 839207, 11 pages.
39. E. El-Meliegy, M. M. Farag, J. C. Knowles, Dissolution and drug release profiles of phosphate glasses doped with high valency oxides, J Mater Sci: Mater Med (2016) 27:108
40. L.É. Uhljar, S.Y. Kan, N. Radacsi, V. Koutsos, P. Szabó-Révész, R. Ambrus, In Vitro Drug Release, Permeability, and Structural Test of Ciprofloxacin-Loaded Nanofibers, Pharmaceutics 13 (2021) 556, 18 pages.
41. N.J. Coleman and L.L. Hench, Gel-derived mesoporous silica reference material for surface analysis by gas sorption. 1. Textural features, Ceram. Int. 26(2) (2000) 171-178.
42. S. Dash, P.N. Murthy, L. Nath, P. Chowdhury, Kinetic modeling on drug release from controlled drug delivery systems, Acta Pol. Pharm., 67(3) (2010 217-223.
43. Higuchi T. Mechanism of sustained action medication. Theoretical analysis of rate of release of solid drugs dispersed in solid matrices, J Pharm Sci. 52 (1963) 1145-9.

Figures

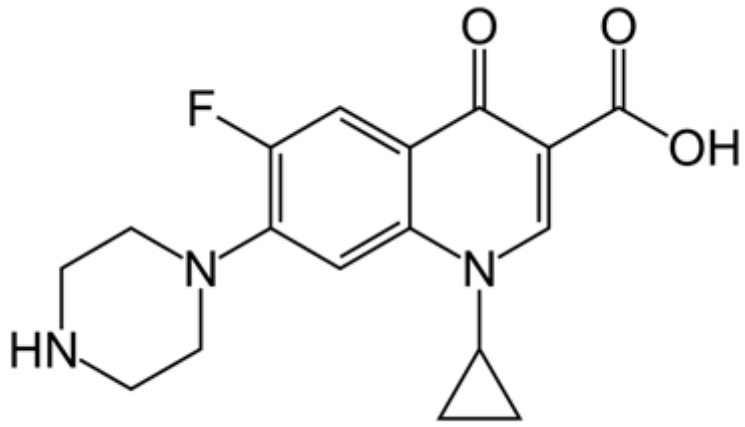

Figure 1

Structure of ciprofloxacin

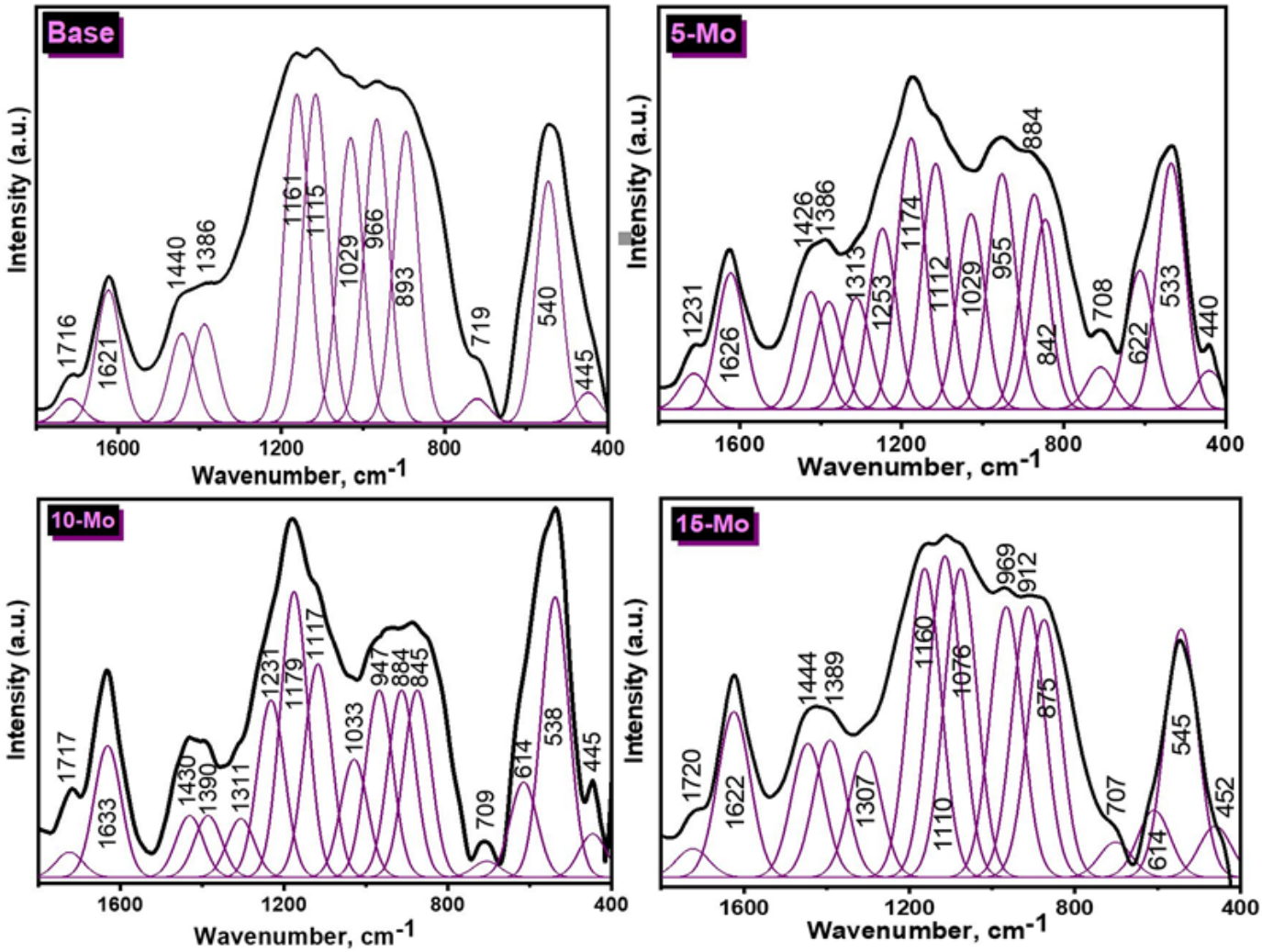

Figure 2

FTIR spectra of undoped and Mo_2O_3 doped glasses before immersion in SBF

Figure 3

FTIR spectra of undoped and Mo_2O_3 doped glasses after immersion in SBF

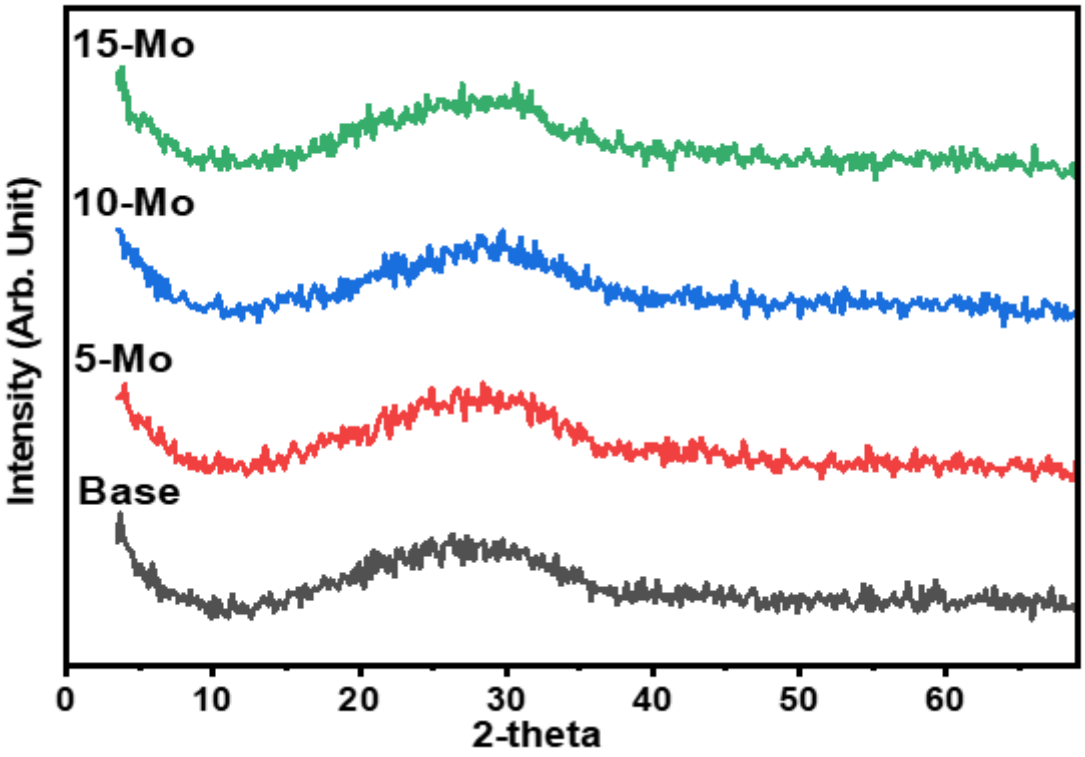

Figure 4

XRD spectra of undoped and Mo_2O_3 doped glasses before immersion

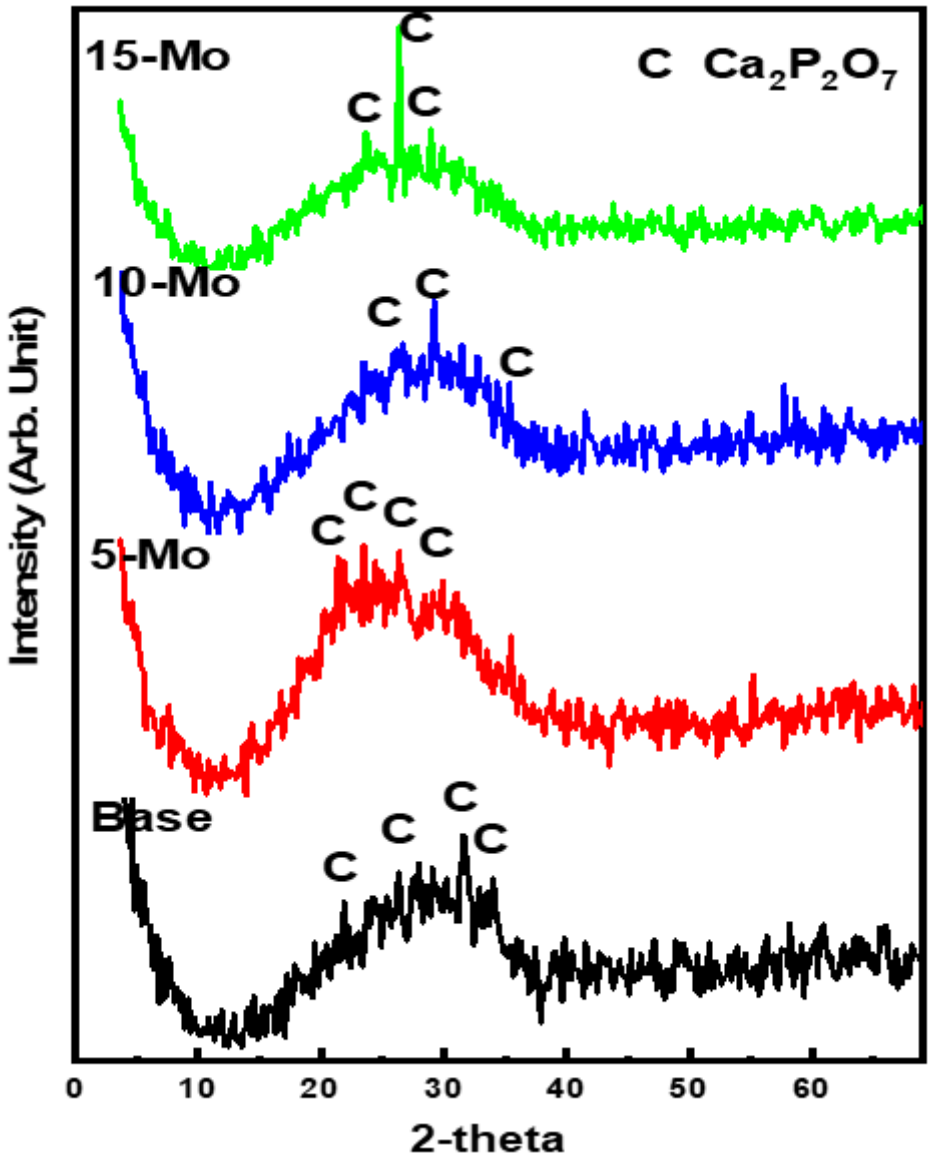

Figure 5

XRD spectra of undoped and MoO_3 doped glasses after immersion for 14 days in SBF

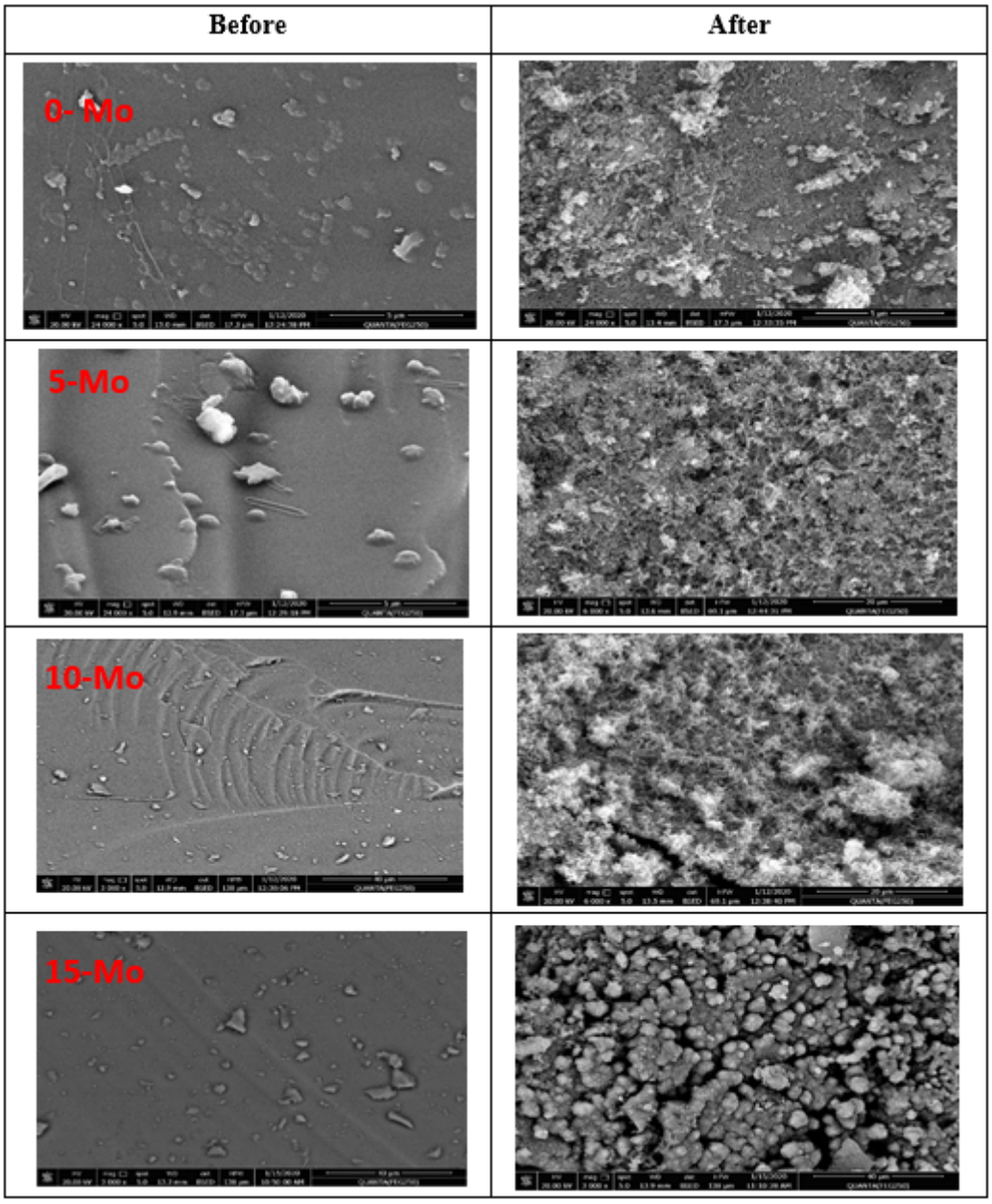

Figure 6

SEM of undoped and Mo_2O_3 doped glasses after immersion in SBF

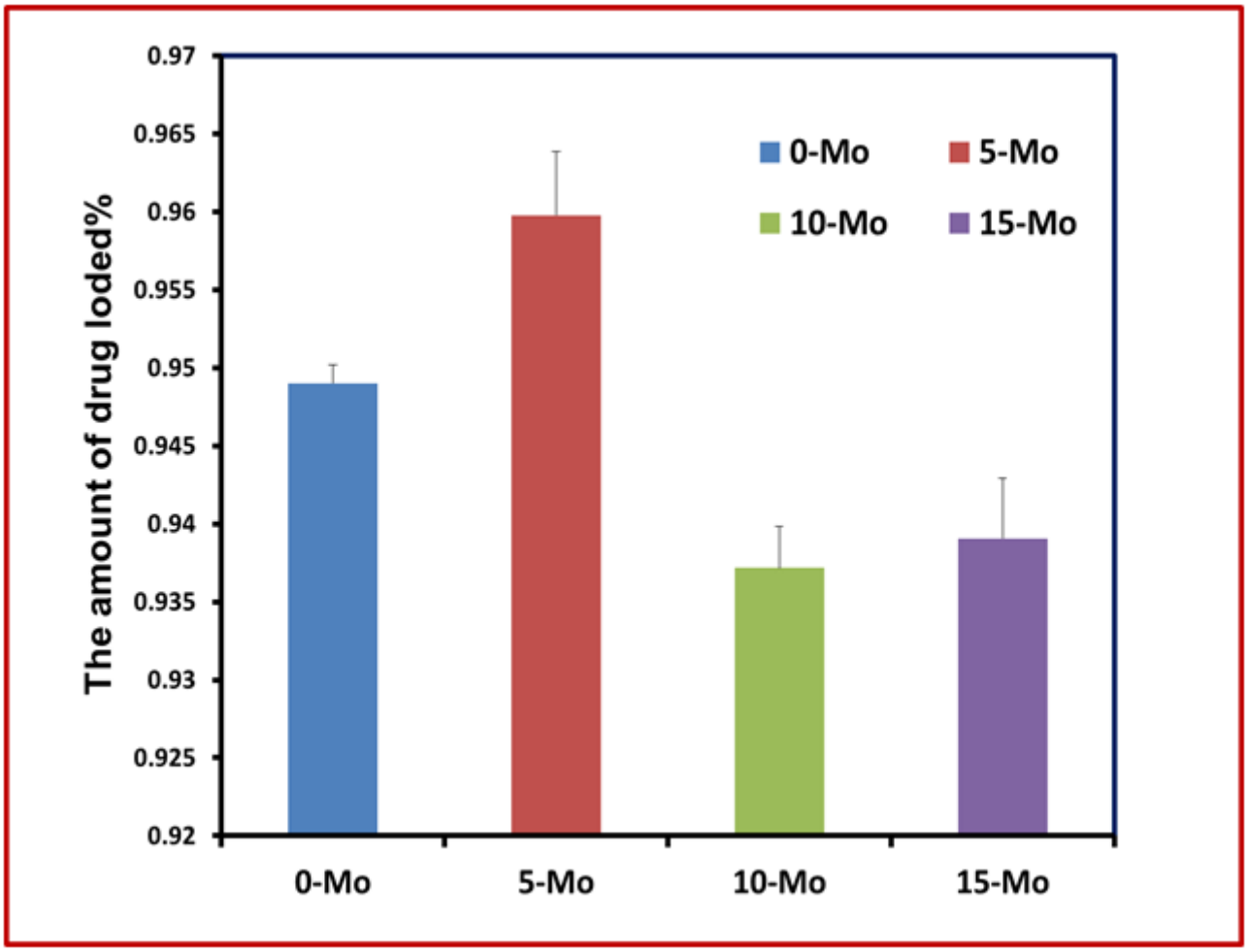

Figure 7

The amount of ciprofloxacin loaded onto glass

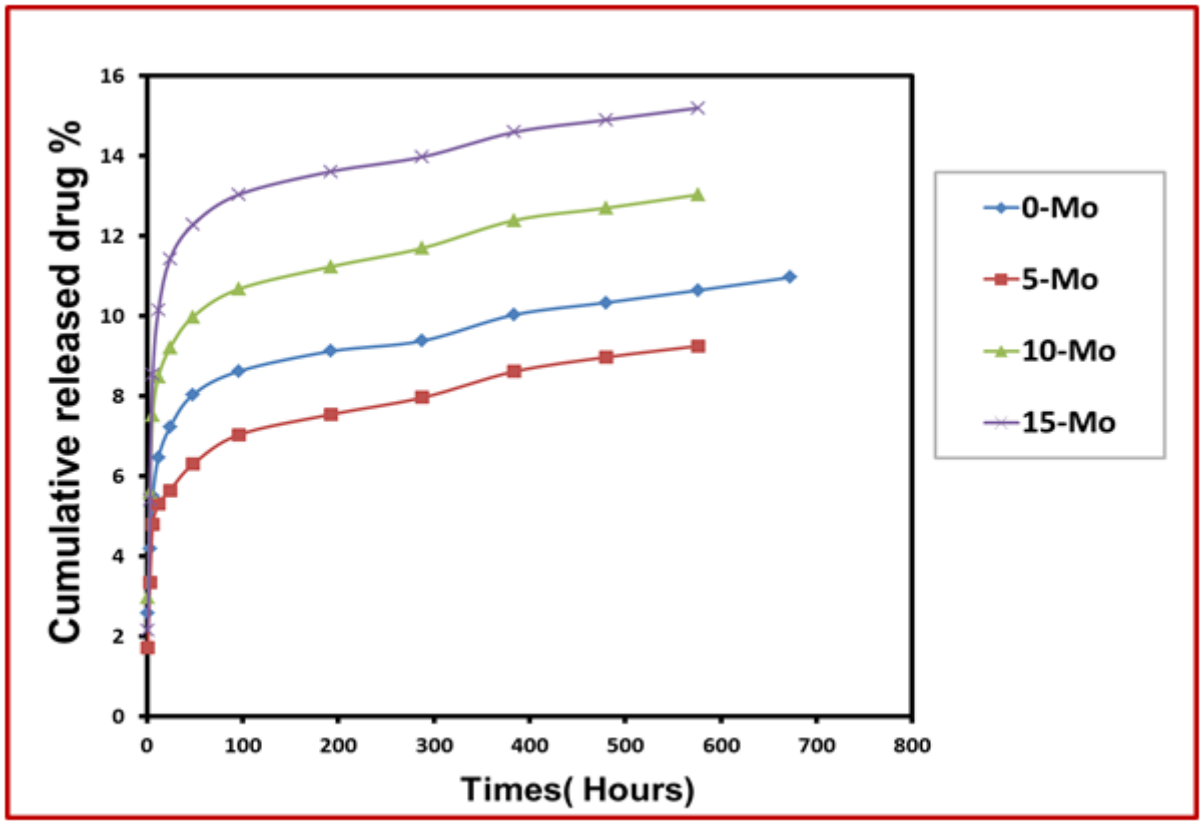

Figure 8

Ciprofloxacin (mg) release profile from studied glasses

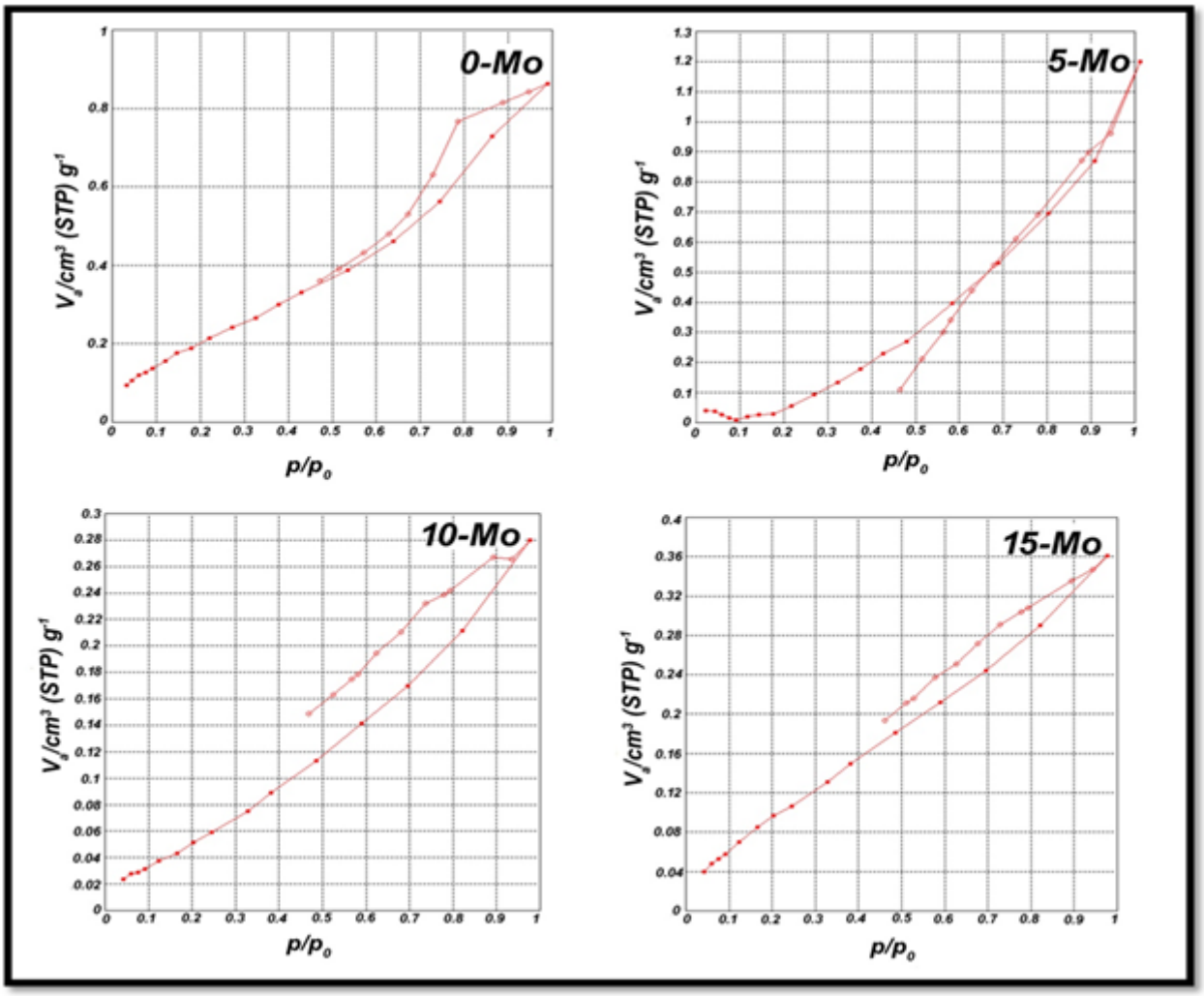

Figure 9

The Nitrogen adsorption–desorption isotherms of samples that correspond to the type IV isotherm according to the IUPAC classification

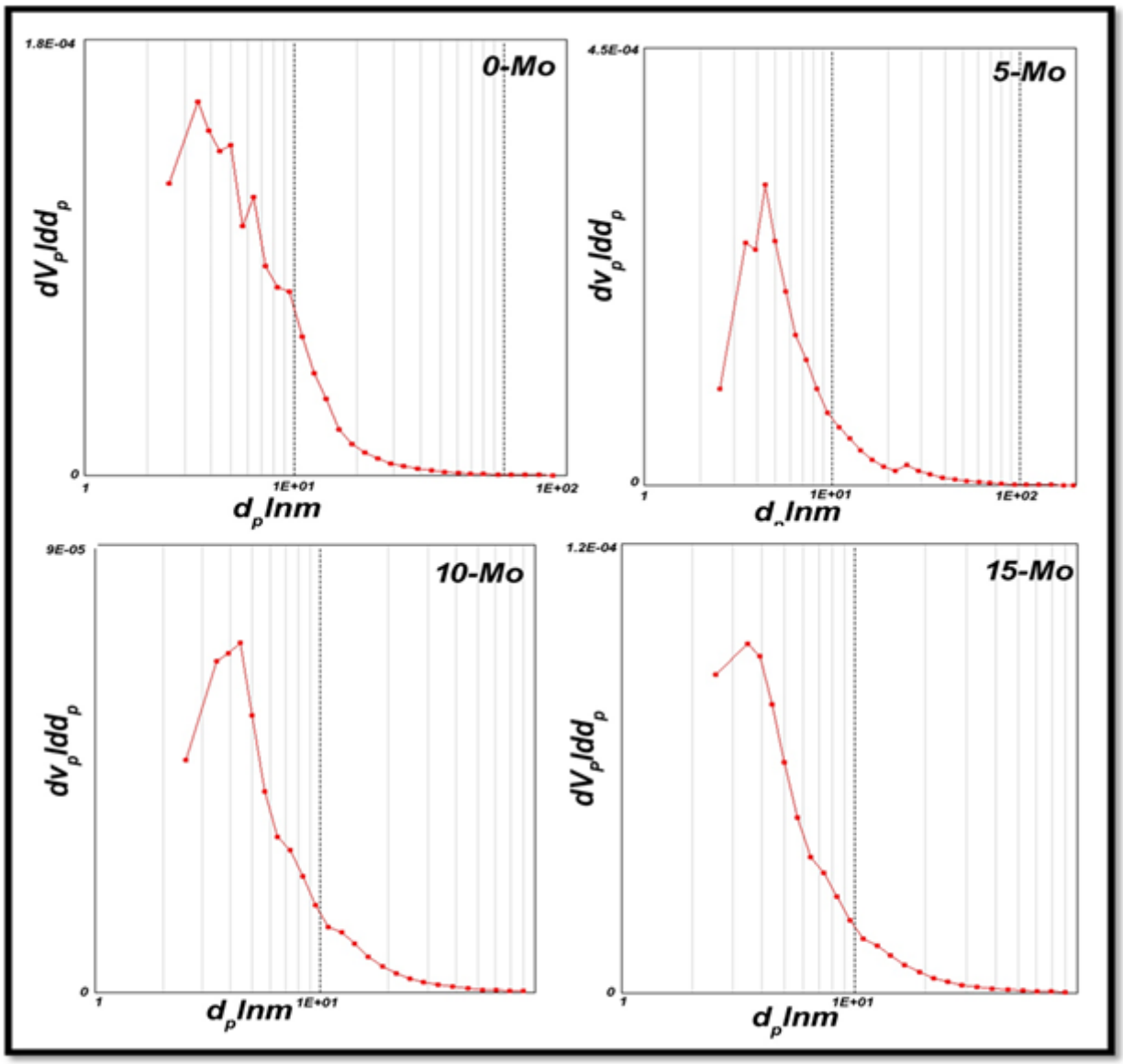

Figure 10

The pore size distributions obtained from the desorption branch of the isotherm following the BJH method for samples

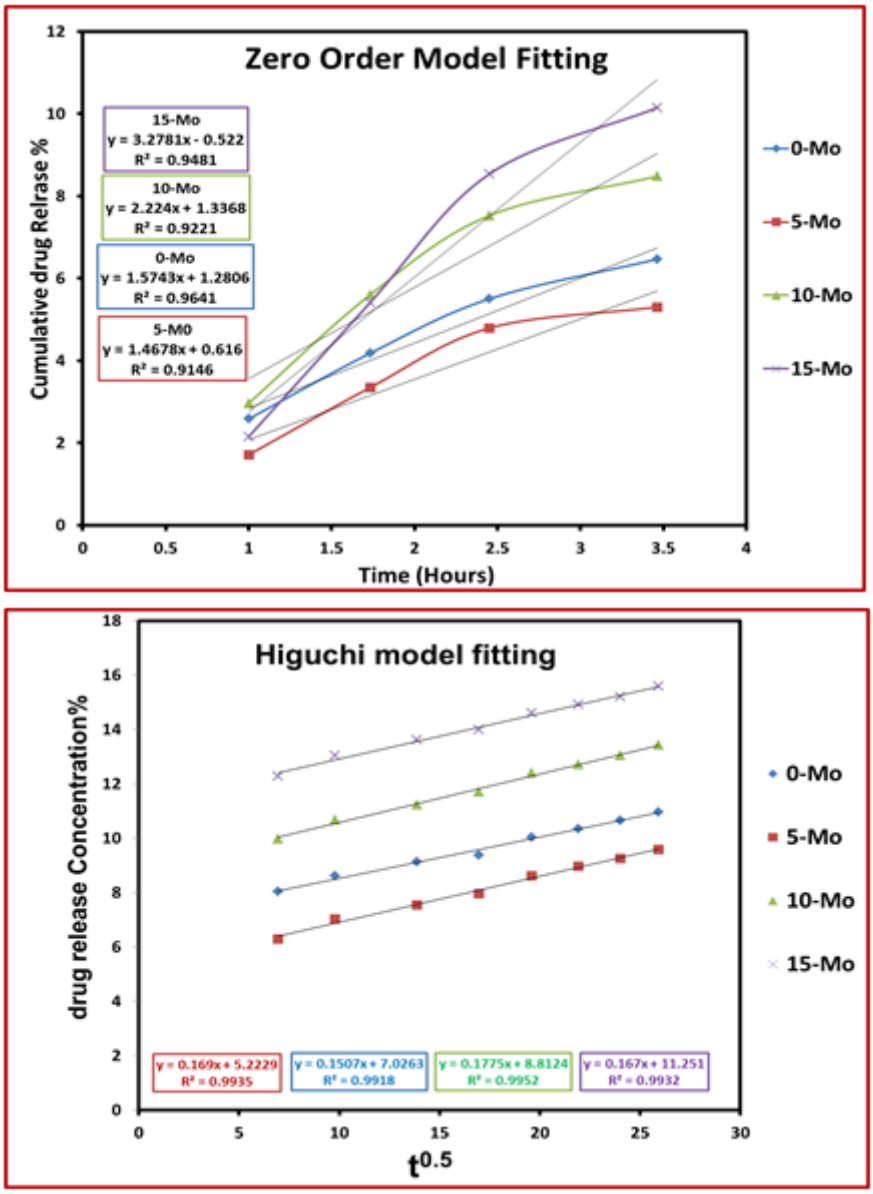

Figure 11

Ciprofloxacin drug release profiles of the different phosphate glasses (0-Mo, 5-Mo, 10-Mo and 15-Mo) using Tris-buffer solution (pH 7.4) as incubating medium, and Zero Order and Higuchi models fitting